QCD thermodynamics with $N_f = 2+1$ near the continuum limit at realistic quark masses

RBC-Bielefeld Collaboration: Takashi Umeda[*]

Brookhaven National Laboratory, Upton, NY 11973, USA
E-mail: `tumeda@bnl.gov`

We report on our study of QCD thermodynamics with $2+1$ flavors of dynamical quarks. In this proceeding we present several thermodynamic quantities and our recent calculation of the critical temperature. In order to investigate the thermodynamic properties of QCD near the continuum limit we adopt improved staggered (p4) quarks coupled with tree-level Symanzik improved glue on $N_t = 4$ and 6 lattices. The simulations are performed with a physical value of the strange quark mass and light quark masses which are in the range of $m_q/m_s = 0.05 - 0.4$. The lightest quark mass corresponds to a pion mass of about 150 MeV.

---

[*]Speaker.

1. Introduction and Lattice Setup

The calculation of QCD thermodynamics from first principle is important for various research areas such as Heavy Ion Phenomenology, Cosmology and Astrophysics. Lattice QCD enables us to carry out such calculations. Especially for HIC phenomenology it is mandatory to improve estimates on some basic thermodynamic quantities which have been obtained in previous lattice calculations. One of the main subjects in our project is the accurate determination of the critical temperature T_c, whose uncertainty, for example, strongly affects the critical energy density ε_c because of its T_c dependence, $\varepsilon_c \sim T_c^4$.

Since thermodynamics of lattice QCD requires huge computational resources, it is difficult to perform an ideal simulation. Recent studies tell us that quark masses and the number of flavors strongly affect thermodynamic quantities [1]. Reliable continuum extrapolations are of tremendous importance as well [2]. Therefore, it is our aim to study QCD thermodynamics with almost realistic quark masses on the QCDOC machine at Brookhaven National Laboratory and the APEnext machine at Bielefeld University. The calculation is performed with $N_f = 2+1$, which means 2 degenerate light quarks and one heavier quark on lattices with $N_t = 4$ and 6. The lightest quark masses of our simulation yields a pion mass of about 150 MeV and a kaon mass of about 500 MeV.

For such calculations we adopt the p4fat3 quark action, which is an improved Staggered quark action [3], with a tree-level improved Symanzik gauge action. By using the p4fat3 action, the free quark dispersion relation has the continuum form up to $O(p^4)$, and the taste symmetry breaking is suppressed by a 3-link fattening term. The action also improves bulk thermodynamical quantities in the high temperature limit [3]. The improvements are essential to control the continuum extrapolation on rather coarse lattices, i.e. $N_t = 4$ and 6. The gauge ensembles are generated by an exact RHMC algorithm [4].

As a status report of the project, in this proceeding, we present several thermodynamic quantities, which are order parameters and their susceptibilities, the static quark potential, and the spatial string tension. In the last section we discuss the critical temperature at the physical point. The details of the critical temperature calculation are given in our recent paper [5].

2. Order Parameters and Susceptibilities

To investigate the QCD critical temperature and phase diagram, order parameters of the QCD transition are indispensable. In the chiral limit the chiral condensate $\langle \bar{\psi}\psi \rangle$ is the order parameter for the spontaneous chiral symmetry breaking of QCD. On the other hand in the heavy quark limit the Polyakov loop $\langle L \rangle$ is the order parameter of the deconfinement phase transition. For finite quark masses, these observables remain good indicators for the (pseudo) critical point. Especially their susceptibilities are useful to determine the critical coupling β_c in numerical simulations.

Figure 1 shows the susceptibilities of the light quark chiral condensate [1] on $8^3 \times 4$ and $16^3 \times 4$ lattices with various quark masses. The peak positions of the susceptibilities define the point of the most drastic change of each order parameter, i.e. the (pseudo) critical point of the QCD transition. The results are interpolated in the coupling β by using the multi-histogram re-weighting technique [6].

---

[1]We always use here the disconnedted part of the chiral susceptibility.
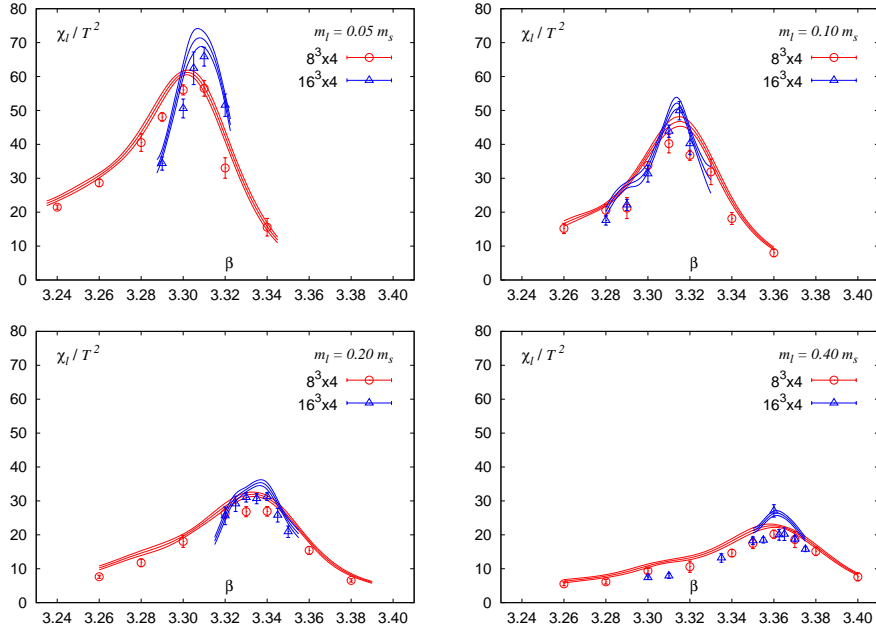
Figure 1: The susceptibility of the light quark chiral condensate on $8^3 \times 4$ and $16^3 \times 4$ lattices. Each panels correspond to results with $\hat{m}_l/\hat{m}_s = 0.05, 0.1, 0.2$ and 0.4 respectively. The lines are calculated by the multi-histogram re-weighting technique.
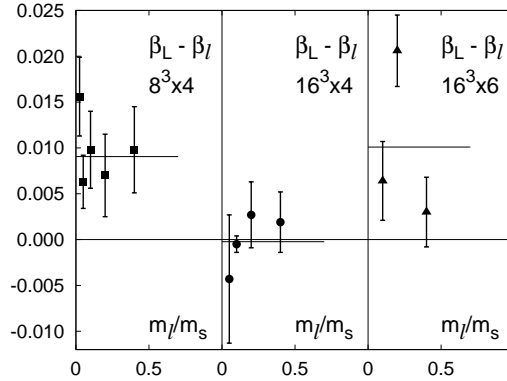

Figure 2: The difference of gauge couplings at the location of peaks in the Polyakov loop and the chiral susceptibilities, $\beta_L - \beta_l$.

The strength of the transition decreases with increasing quark masses, this is reflected in the decreasing peak height of the chiral susceptibilities. We calculate these susceptibilities on lattices with aspect ratios of $N_s/N_t = 2$ and 4. Since we see a rather small volume dependence the results suggest that the transition is in fact not a true phase transition in the thermodynamic sense but a rapid crossover.

Figure 2 (left) shows the difference in the peak position of the chiral and Polyakov loop susceptibilities. The differences are small and almost identical at the aspect ratio of $N_s/N_t = 4$, which
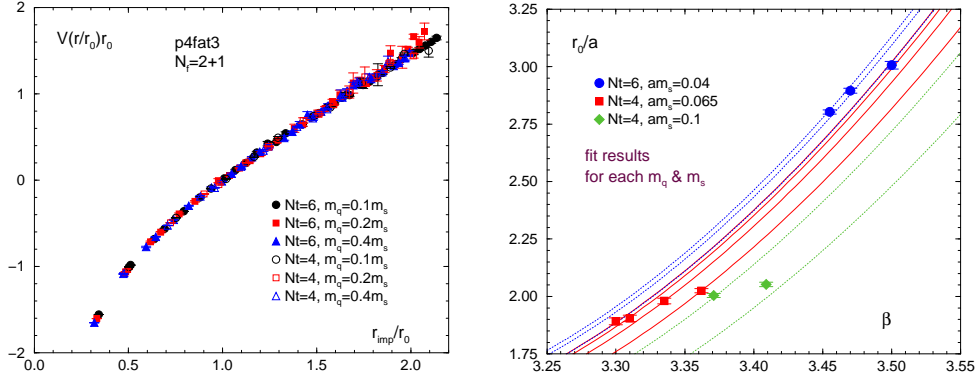
Figure 3: Heavy quark potentials scaled by r_0 for various cut-offs and quark masses (left) and a global fit of r_0/a with the RG inspired ansatz Eq.(3.3) (right).

indicates the chiral and deconfinement phase transition occur at almost the same temperature. The discrepancy between the peak positions shrinks with increasing volume.

3. Scale Setting and the Heavy Quark Potential

The lattice scale is determined by the heavy quark potential $V(r)$ which is extracted from Wilson loops. The Wilson loop expectation values are calculated on $16^3 \times 32$ lattices with APE smearing in spatial direction. The spatial path in a loop is determined by the Bresenham algorithm [8]. We calculate the string tension, σ and Sommer scale r_0, which is defined [7] as the distance where the corresponding force of the static quark potential matches a certain value suggested by phenomenology: $r^2 \frac{\partial V}{\partial r}|_{r=r_0} = 1.65$. To remove short range lattice artifacts we use the improved distance, r_{imp}, which is defined as

$$\frac{1}{4\pi r_{imp}} \equiv \int \frac{d^3k}{(2\pi)^3} \frac{e^{ikr}}{4\sum_i(\sin^2\frac{k_i}{2}) + \frac{1}{3}\sin^4\frac{k_i}{2}}. \tag{3.1}$$

In our lattice setup, we find almost no mass and cutoff dependence in the potential scaled by r_0 at $N_\tau = 4$ and 6 (Fig.2(left)). As discussed in previous studies [9], we also find no string breaking effects even at large r. To estimate systematic uncertainties of the potential fit, we performed several types of fits, e.g. different fit-ranges in r and fit-forms (3 & 4 params. fits),

$$V(r) = C + \frac{\alpha}{r_{imp}} + \sigma r_{imp}, \quad V(r) = C + \frac{\alpha}{r} + \sigma r + d(\frac{\alpha}{r_{imp}} - \frac{\alpha}{r}). \tag{3.2}$$

The differences in the mean values of the fits are taken into account as a systematic uncertainty of the scale setting.

We have determined the scale parameter r_0 in units of the lattice spacing for 9 different parameter sets. This allows to interpolate between different values of the gauge coupling and quark masses. We use a renormalization group inspired ansatz [10] which takes into account the quark mass dependence of r_0/a [11] and which approaches, in the weak coupling limit, the 2-loop β-function for three massless flavors,

$$(r_0/a)^{-1} = R(\beta)(1 + B\hat{a}^2(\beta) + C\hat{a}^4(\beta))e^{A(2\hat{m}_l + \hat{m}_s) + D}. \tag{3.3}$$
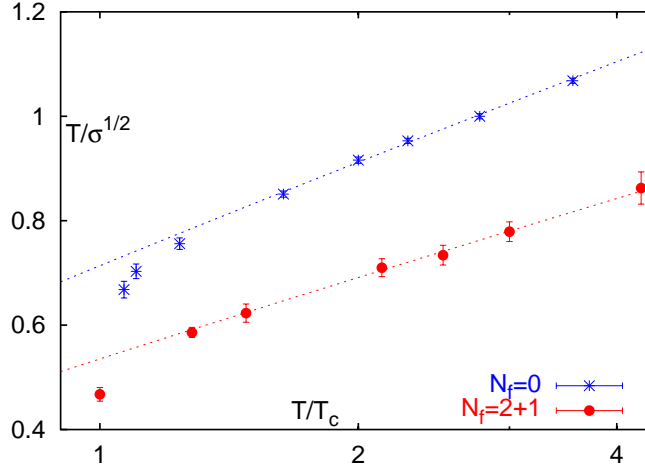
4

Figure 4: Temperature dependence of the spatial string tension for $N_f = 0$ and $N_f = 2+1$. Both dotted lines are fits with Eq. (4.1). Note, that the scale on the horizontal axis is logarithmic.

Here $R(\beta)$ denotes the 2-loop β-function and $\hat{a}(\beta) = R(\beta)/R(\bar{\beta})$ with $\bar{\beta} = 3.4$ chosen as an arbitrary normalization point.

4. Spatial String Tension

Let us now discuss the calculation of the spatial string tension which is important to verify the theoretical concept of dimensional reduction at high temperatures. The spatial string tension is extracted from the spatial static quark "potential" (from spatial Wilson loops). We use the same analysis technique as for the usual (temporal) static quark potential.

At high temperature, the spatial string tension $\sigma_s(T)$ is expected to behave like

$$\sqrt{\sigma_s(T)} = c g^2(T) T. \tag{4.1}$$

Here $g^2(T)$ is the temperature dependent coupling constant from the 2-loop RG equation,

$$g^{-2}(T) = 2b_0 \ln \frac{T}{\Lambda_\sigma} + \frac{b_1}{b_0} \ln \left(2\ln \frac{T}{\Lambda_\sigma} \right). \tag{4.2}$$

If dimensional reduction works, the parameter "c" should be equal to the 3-dimensional string tension and should be flavor independent.

Our 2+1 flavor result yields $c = 0.587(41)$ and $\Lambda_\sigma/T_c = 0.114(27)$, obtained by a fit with Eq.(4.1). On the other hand, we plot in Fig. 4 also the quenched result [12] which gives $c = 0.566(13)$ and $\Lambda_\sigma/T_c = 0.104(9)$. We thus find that the parameter "c" is – within statistical errors – independent on the number of dynamical flavors and that dimensional reduction works well even for $T = 2T_c$. This analysis can and will be refined in the future by taking into account higher order corrections to Eq.(4.1) [13].
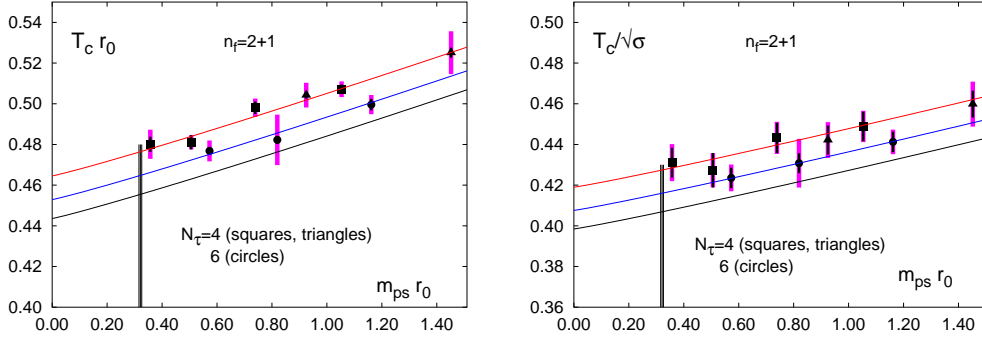
Figure 5: $T_c r_0$ (left) and $T_c/\sqrt{\sigma}$ (right) as a function of $m_{ps}r_0$ on lattices with temporal extent $N_\tau = 4$, $\hat{m}_s = 0.065$ (squares) and $\hat{m}_s = 0.1$ (triangles) as well as for $N_\tau = 6$, $\hat{m}_s = 0.04$ (circles). Thin error bars represent the statistical and systematic error on r_0/a and $\sqrt{\sigma}a$. The broad error bar combines this error with the error on β_c. The vertical line shows the location of the physical value $m_{ps}r_0 = 0.321(5)$ and its width represents the error on r_0. The three parallel lines show results of fits based on Eq. (5.1) with $d = 1.08$ for $N_\tau = 4$, 6 and $N_\tau \to \infty$ (top to bottom).

5. The transition temperature

Finally I discuss the transition temperature in QCD, which is one of the most important subjects in our project. In sect.2 we have determined the critical β at each N_τ and for several quark masses. At these couplings we performed zero temperature calculations of the static quark potential. The scale settings at each critical β provide each values for the critical temperature. We thus can extrapolate T_c to the chiral limit as well as to the physical point by using a scaling ansatz. In the zero temperature calculations the actual β is sometimes slightly different from our final result on the critical β. The differences are corrected by using Eq.3.3. Furthermore a systematic error in the critical β, e.g. $\beta_L - \beta_l$ at $N_\tau = 6$ in Fig.2, is also taken into account in the critical temperature.

In Fig. 5 we plot the critical temperature in unit of the Sommer scale (left) and the string tension (right) as function of the pion mass m_{PS} (also in units of the Sommer scale). Thin error bars represent the statistical and systematic error on r_0/a and $\sqrt{\sigma}a$. The broad error bar combines this error with the error on β_c. We perform a combined chiral and continuum extrapolation of T_c by using the ansatz, e.g. in unit of the Sommer scale,

$$T_c r_0 = \left[T_c r_0\right]_{\text{cont}}^{\text{chiral}} + A(m_\pi r_0)^d + B/N_\tau^2, \tag{5.1}$$

where A and B are free fit parameters. If the QCD transition is second order in the chiral limit the transition temperature is expected to depend on the quark mass as $\hat{m}_l^{1/\beta\delta}$, which corresponds to $d \simeq 1.08$ in Eq. 5.1, by the fact that one expects a critical point in the chiral limit which is in the $O(4)$-universality class. If, on the other hand, the transition becomes first order for small quark masses, the transition temperature will depend linearly on the quark mass, i.e. $d = 2$. Using the fit form ansatz 5.1 we can determine the transition temperature at the physical point, which is defined as $m_{ps}r_0 \equiv 0.321(5)$,

$$T_c r_0 = 0.457(7)_{-3}^{+12}, \quad T_c/\sqrt{\sigma} = 0.408(8)_{-1}^{+3}, \tag{5.2}$$

where the central value is given for fits with $d = 1.08$ and the lower and upper systematic error correspond to $d = 1$ and $d = 2$, respectively.

In order to convert T_c to physical units, we use the scale parameter, $r_0 = 0.469(7)$ fm, deduced from the bottomonium level splitting using NRQCD [14]. Finally we obtain the transition temperature in QCD at the physical point, $T_c = 192(7)(4)$ MeV, where the statistical error includes the errors given in Eq. 5.2 as well as the uncertainty in the value of r_0 and the second error reflects our estimate of a remaining systematic error on the extrapolation to the continuum limit. The value of the critical temperature obtained here is about 10% larger than the frequently quoted value ~ 175 MeV. We note that this larger value mainly results from the value for r_0 used in our conversion to physical scales.

The analysis presented here leads to a value for the critical temperature with about 5% statistical and systematic errors. It clearly is desirable to confirm our estimate of the remaining systematic errors through an additional calculation on an even finer lattice. Furthermore, it is desirable to verify this result through calculations using other $T = 0$ scales and to explore other discretization schemes for the fermion sector of QCD and to also obtain a reliable independent scale setting for the transition temperature from an observable not related to properties of the static quark potential.

Acknowledgments

References

[1] F. Karsch, E. Laermann and A. Peikert, Nucl. Phys. B **605**, 579 (2001).

[2] A. Ali Khan *et al.* [CP-PACS collaboration], Phys. Rev. D **64**, 074510 (2001).

[3] U. M. Heller, F. Karsch and B. Sturm, Phys. Rev. D **60**, 114502 (1999).

[4] M. A. Clark, A. D. Kennedy and Z. Sroczynski, Nucl. Phys. Proc. Suppl. **140**, 835 (2005).

[5] M. Cheng *et al.*, Phys. Rev. D **74**, 054507 (2006), [arXiv:hep-lat/0608013].

[6] A. M. Ferrenberg and R. H. Swendsen, Phys. Rev. Lett. **61** (1988) 2635.

[7] M. Guagnelli, R. Sommer and H. Wittig [ALPHA collaboration], Nucl. Phys. B **535**, 389 (1998).

[8] B. Bolder *et al.*, Phys. Rev. D **63**, 074504 (2001).

[9] S. Aoki *et al.* [CP-PACS Collaboration], Phys. Rev. D **60**, 114508 (1999).

[10] C. Allton, Nucl. Phys. B [Proc. Suppl.] **53**, 867 (1997).

[11] C. Bernard *et al.* [MILC Collaboration], Phys. Rev. D **71**, 034504 (2005).

[12] G. Boyd et al., Nucl. Phys. B **469**, 419 (1996).

[13] Y. Schroder and M. Laine, PoS **LAT2005**, 180 (2006)

[14] A. Gray et al., Phys. Rev. D **72**, 094507 (2005)